EPJ B
Condensed Matter and Complex Systems
www.epj.org

Eur. Phys. J. B **62**, 319–326 (2008) DOI: 10.1140/epjb/e2008-00162-5

Global firing induced by network disorder in ensembles of active rotators

C.J. Tessone, D.H. Zanette and R. Toral

EDP SCIENCES
Società Italiana di Fisica
Springer

Eur. Phys. J. B **62**, 319–326 (2008)
DOI: 10.1140/epjb/e2008-00162-5

THE EUROPEAN PHYSICAL JOURNAL B

Global firing induced by network disorder in ensembles of active rotators

C.J. Tessone[1,a], D.H. Zanette[2], and R. Toral[3]

[1] Chair of Systems Design, ETH Zurich, Kreuzplatz 5, 8032 Zurich, Switzerland
[2] Consejo Nacional de Investigaciones Científicas y Técnicas, Centro Atómico Bariloche and Instituto Balseiro, 8400 Bariloche, Río Negro, Argentina
[3] IFISC (Instituto de Física Interdisciplinar y Sistemas Complejos), CSIC-UIB, Ed. Mateu Orfila, Campus UIB, 07122 Palma de Mallorca, Spain

Received 17 October 2007 / Received in final form 28 February 2008
Published online 19 April 2008 –

Abstract. We study the influence of repulsive interactions on an ensemble of coupled excitable rotators. We find that a moderate fraction of repulsive interactions can trigger global firing of the ensemble. The regime of global firing, however, is suppressed in sufficiently large systems if the network of repulsive interactions is fully random, due to self-averaging in its degree distribution. We thus introduce a model of partially random networks with a broad degree distribution, where self-averaging due to size growth is absent. In this case, the regime of global firing persists for large sizes. Our results extend previous work on the constructive effects of diversity in the collective dynamics of complex systems.

PACS. 05.45.Xt Synchronization; coupled oscillators – 05.45.-a Nonlinear dynamics and chaos – 89.75.Fb Structures and organization in complex systems

1 Introduction

Noise and disorder can have a variety of effects on the collective dynamics of complex systems such as biological populations, chemical reactions, oscillator ensembles, among others. Somehow paradoxically, such effects often play a constructive role in inducing coherent behaviour in the system [1–3]. An already classical example is the phenomenon of stochastic resonance, where noise of appropriate intensity enhances the response of a system to an oscillatory external forcing [4]. A similar effect in an extended system can be caused by the presence of some degree of heterogeneity amongst the constituents, a phenomenon named *diversity-induced resonance* [5]. Also, a certain degree of structural disorder in a network can make the propagation of information considerably more efficient [6].

It was recently shown that, in an ensemble of coupled excitable rotators, noise and disorder are able to trigger global firing [7]. During these events, a substantial fraction of the ensemble is excited almost synchronously, so that the joint firing of all those elements gives rise to a collective process which can be detected at macroscopic level. This phenomenon has been observed under the action of additive noise, when stochastic terms are added to the evolution equations, or under ensemble heterogeneity, when the parameters that define the individual dynamics of the rotators differ all over the ensemble. Since these previous studies considered all-to-all (global) homogeneous coupling between elements, the effect of disorder in their interaction network was not analysed.

Global coupling has frequently been invoked as an analytically tractable interaction pattern for which several systems are completely solvable [8]. In real situations, however, the interaction pattern is usually heterogeneous, with different weights for each pair of interacting elements. Some systems, such as neural networks, even require the consideration of interactions of different signs, to account for excitatory and inhibitory coupling [9–11]. Interaction patterns with attractive and repulsive weights in ensembles of coupled dynamical elements was first addressed by Daido [12–14]. Their effect on the stability of synchronisation in an ensemble of phase oscillators, in terms of the relative number and strength of positive and negative couplings, has been studied recently [16]. It was found that a certain fraction of sufficiently strong repulsive interactions, distributed at random over the interaction pattern, is able to induce a transition from the highly coherent state of full synchronisation, where all elements oscillate in phase, to an unsynchronised state. Recently, in a different context, a condition for synchronisability of heterogeneous networks with attractive interactions was found [15].

The presence of randomly scattered negative couplings in the interaction pattern of an ensemble of dynamical

[a] e-mail: tessonec@ethz.ch

elements is a source of structural disorder, complementary to noise and to the heterogeneity of the ensemble. It is therefore natural to study its effects on the collective dynamics of coupled excitable elements and, in particular, on the phenomenon of global firing. This is our aim in this paper, which is organised as follows: in Section 2, we introduce the model of coupled excitable rotators, and the order parameters used in the characterisation of the collective macroscopic behaviour of the ensemble. Next, in Section 3, we consider the case when repulsive interactions form a fully random (Erdös-Rényi) network. In this case, global firing is observed for finite-size systems but, due to self-averaging in the degree distribution of fully random networks, the phenomenon is suppressed in the limit of infinitely large ensembles. Thus, in Section 4, we introduce a model of partially random networks where the relative dispersion of the degree distribution does not depend on the size. When repulsive interactions are distributed over such a network, global firing is found to persist for large systems. Our conclusions are discussed in the final Section 5.

2 Model and order parameters

We consider an ensemble of coupled active rotators [17] with individual phases $\phi_j(t) \in [0, 2\pi)$, $j = 1, \ldots, N$, whose dynamics is given by

$$\dot{\phi}_j = \omega - \sin\phi_j + \frac{C}{N}\sum_{k=1}^{N} W_{kj}\sin(\phi_k - \phi_j). \qquad (1)$$

The coupling strength is measured by the parameter $C \geq 0$, and each factor W_{kj} weights the interaction of a specific rotator pair. These weights are symmetric, $W_{kj} = W_{jk}$. Attractive and repulsive interactions are characterised, respectively, by $W_{kj} > 0$ and $W_{kj} < 0$.

The natural frequency $\omega > 0$ is the same for all rotators. For $\omega > 1$ and in the absence of coupling, the individual dynamics is oscillatory, with an actual frequency $\omega' = \sqrt{\omega^2 - 1}$. The case $\omega < 1$ corresponds to excitable individual dynamics: for $C = 0$, the phase ϕ_j of each rotator has two fixed points, one of them stable ($\phi_s < \pi/2$) and the other unstable ($\phi_u > \pi/2$), at the two solutions of $\sin\phi_j = \omega$. A perturbation of the stationary stable solution which overcomes the unstable fixed point ϕ_u gives rise to the *firing* of the rotator, in the form of a long phase excursion which finally returns to the rest state ϕ_s. Throughout this paper we focus the attention on the excitable regime $\omega < 1$.

In our model noise is absent and, for $C = 0$, individual rotators are identical. Diversity is thus restricted to disorder in the interaction network, through the weights W_{kj}. Our main aim is, in fact, to analyse the effects of this source of diversity in the collective dynamics of the system.

If all the phases ϕ_j coincide with one of the two fixed points of the individual dynamics, either ϕ_s or ϕ_u, the ensemble is in a stationary state – which we refer to as *full synchronisation* – for any value of C. If the weights W_{kj} are positive for all k and j, the fully synchronised state where all the rotators are in the rest state, $\phi_j = \phi_s$ for all j, is stable. The stability of this collective rest state can break down, however, in the presence of repulsive interactions, when some of the weights W_{kj} are negative and their absolute value is large enough. In this situation, generally, the ensemble does not reach an asymptotic stationary state. Individual phases can now rotate irregularly around their whole domain and, as we show below, a regime of global firing – where a fraction of the ensemble is collectively entrained into long excursions from the unstable fixed point to the rest state – becomes possible.

The collective behaviour of the rotator ensemble, including possible transitions between different dynamical regimes, is well characterised by a set of order parameters defined in terms of the individual phases $\phi_j(t)$. First, we take the average of the imaginary phase exponentials

$$\rho(t)\exp[i\Psi(t)] = \frac{1}{N}\sum_{j=1}^{N}\exp[i\phi_j(t)], \qquad (2)$$

and compute the Kuramoto order parameter as $\rho \equiv \langle\rho(t)\rangle$, where $\langle\cdot\rangle$ stands for the time average over a long interval [8]. This parameter is a direct measure of the degree of synchronisation attained by the ensemble. For a fully synchronised state we have $\rho = 1$, whereas $\rho \sim 1/\sqrt{N}$ for a state where phases are uniformly distributed over $[0, 2\pi)$.

The Kuramoto order parameter cannot discern between the case where phases are synchronised at a fixed point, as at the rest state ϕ_s, and the case where they rotate coherently, as expected to occur in a regime of global firing. To discriminate between static and dynamic entrainment, we apply the order parameter introduced by Shinomoto and Kuramoto [17]:

$$\zeta = \langle|\rho(t)\exp[i\Psi(t)] - \langle\rho(t)\,\exp[i\Psi(t)]\rangle|\rangle\,. \qquad (3)$$

This parameter differs from zero for synchronous firing only.

A third order parameter, frequently used in the analysis of stochastic transport [18], is the current

$$J = \frac{1}{N}\sum_{j=1}^{N}\left\langle\dot{\phi}_j(t)\right\rangle. \qquad (4)$$

It measures the level of (not necessarily synchronised) firing over the whole ensemble.

3 Erdös-Rényi networks of repulsive links

First, we consider an ensemble of rotators governed by equation (1), whose interaction weights are distributed at random according to the following prescription:

$$W_{kj} = \begin{cases} 1 \text{ with probability } 1 - p_d, \\ -\kappa \text{ with probability } p_d. \end{cases} \qquad (5)$$

The coefficient $\kappa > 0$ measures the relative strength of repulsive and attractive interactions, and the probability p_d fixes the expected fraction of negative weights. Repulsive interactions define a network which, with the prescription of equation (5), has the same structure as an Erdös-Rényi random network [19–21]. On the average, the network of repulsive interactions has $p_d N(N-1)/2$ links. We call $\mathcal{N}_j$ the set of neighbours of rotator j in that network. The mean number of rotators in $\mathcal{N}_j$ is $p_d(N-1)$, and the expected dispersion around this average is of order $\sqrt{N}$, so that the relative dispersion decreases with the size as $1/\sqrt{N}$.

It is useful to rewrite equation (1) in terms of the quantities $\rho(t)$ and $\Psi(t)$ introduced in equation (2), as

$$\dot{\phi}_j = \omega - \sin\phi_j + C\rho\,\sin(\Psi - \phi_j) - \frac{C(1+\kappa)}{N}\sum_{k\in\mathcal{N}_j}\sin\left(\phi_k - \phi_j\right). \qquad (6)$$

This equation describes the evolution of $\phi_j(t)$ as governed by the interaction with a single (mean-field) oscillator with phase $\Psi(t)$ with an effective coupling strength $C\rho(t)$ plus a negative contribution with coupling $C(1+\kappa)$ from the neighbourhood of rotator j in the network of repulsive links.

3.1 Stability of the fully synchronised state

As advanced above, in the presence of repulsive interactions, the state of full synchronisation may be unstable. The stability condition can be obtained from linearisation of equation (6). Writing $\phi_j(t) = \phi_s + \delta_j(t)$, we get for the deviations from the fixed point the equations

$$\dot{\delta}_j = -\sqrt{1-\omega^2}\,\delta_j - C\delta_j - \frac{C(\kappa+1)}{N}\sum_{k\in\mathcal{N}_j}(\delta_k - \delta_j). \qquad (7)$$

Full synchronisation is stable if all the eigenvalues of the matrix

$$\mathbb{J} = -\left(\sqrt{1-\omega^2} + C\right)\mathbb{I} - \frac{C(\kappa+1)}{N}(\mathbb{M} - \mathbb{N}) \qquad (8)$$

are negative or have negative real parts. Here, $\mathbb{I}$ is the identity matrix, $\mathbb{M} = \{M_{kj}\}$ is the adjacency matrix of the network of repulsive links (defined as $M_{kj} = 1$ if there is a repulsive link between rotators k and j, and $M_{kj} = 0$ otherwise), and $\mathbb{N} = \{N_{kj}\}$ is a diagonal matrix, where $N_{jj} \equiv k_j = \sum_i M_{ij}$ is the number of rotators in $\mathcal{N}_j$ – namely, the degree of site j.

Whether the stability condition for full synchronisation is fulfilled or not depends on the specific realisation of the network of repulsive links. Even for the same probability p_d, and for fixed values of C, ω and κ, the stability of full synchronisation depends on the particular distribution of negative weights. The uppermost panel of Figure 1 shows numerical results for the fraction f_d of realisations of the network of repulsive links for which full synchronisation is unstable, as a function of p_d. As expected, f_d grows as the number of repulsive links increases. Different curves correspond to different system sizes N.

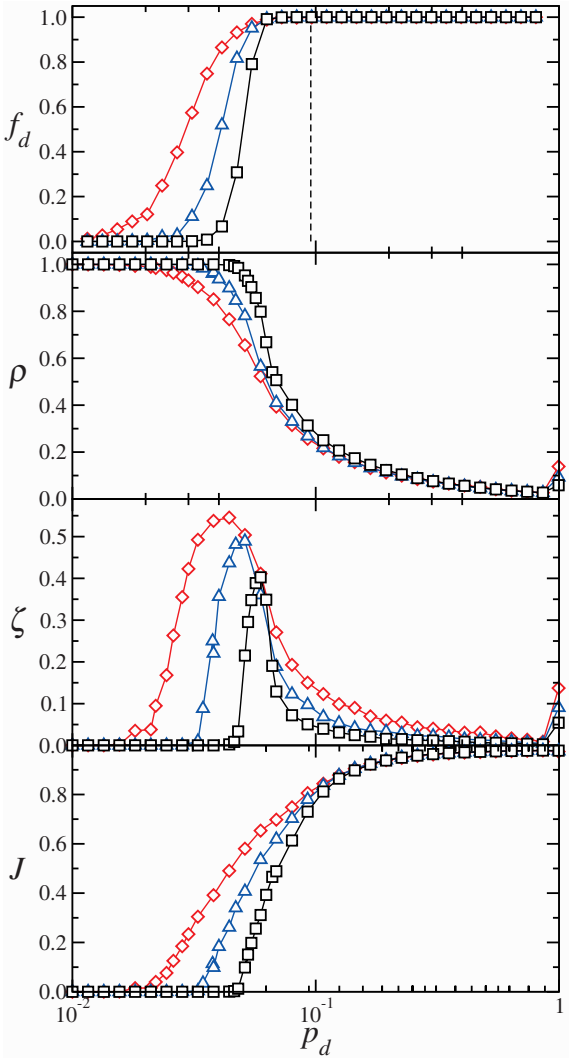

Fig. 1. Uppermost panel: fraction f_d of realisations of the network of repulsive links for which the fully synchronised state is unstable, as a function of the probability p_d, over series of 10^3 realisations. From left to right: $N = 50$ ($\diamond$), 100 ($\triangle$) and 200 ($\square$). The other parameters are $C = 4$, $\kappa = 10$, and $\omega = 0.98$. The vertical dotted line stands for the theoretical transition point, $p_d^* \approx 9.54 \times 10^{-2}$, for an infinitely large ensemble. The three lower panels show the Kuramoto order parameter ρ, the Shinomoto-Kuramoto order parameter ζ, and the current J, for the same realisations.

Numerical results suggest that, for large N, there is a sudden transition from $f_d = 0$ to 1 at a given value p_d^* of the probability p_d. An analytical estimate of p_d^* can be obtained from the assumption that the number of neighbours in the network of repulsive links is the same for all rotators, i.e. that the number of rotators in $\mathcal{N}_j$ is the same for all j. This approximation improves as N grows, because – as stated above – the relative dispersion in the number of rotators in $\mathcal{N}_j$ decreases as $1/\sqrt{N}$. It implies

that the matrix $\mathbb{J}$ can be written as

$$\mathbb{J} = -\left(\sqrt{1-\omega^2} + C - C(\kappa+1)p_d\right)\mathbb{I} - \frac{C(\kappa+1)}{N}\mathbb{M}. \quad (9)$$

For $N \to \infty$, the coefficient in front of the matrix $\mathbb{M}$ tends to zero, suggesting that its contribution to $\mathbb{J}$ can be neglected in that limit. This intuitive argument implies that the point at which the maximum eigenvalue becomes positive for $N \to \infty$ is

$$p_d^* = \frac{C + \sqrt{1-\omega^2}}{C(1+\kappa)}. \quad (10)$$

A more rigorous argument, confirming this critical value for p_d^*, can be obtained from exact bounds for the eigenvalues of the matrix $\mathbb{J}$ in equation (8) coming from the so-called semicircle law [22], applied to matrices $\mathbb{M}$ and $\mathbb{N}$ [16]. The vertical dotted lines in the uppermost panel of Figure 1 stands for this critical value p_d^*.

Close inspection of the destabilisation of full synchronisation reveals that this transition is triggered by the behaviour of the rotator j^* with the largest number of repulsive links – as also observed to occur in ensembles of coupled phase oscillators [16]. For a given value of κ, as the fraction p_d of repulsive links grows, the fixed point ϕ_s first ceases to be a stable state for ϕ_{j^*}. An arbitrarily small deviation in ϕ_{j^*} leads to a different equilibrium point, and full synchronisation breaks down, even when other rotators may remain mutually synchronised. Thus, while varying κ, the transition to full synchronisation occurs via clustering of those nodes with the lowest number of repulsive links. For small sizes N, the value of p_d at which the rotator j^* attains the number of negative interaction weights which makes full synchronisation unstable depends sensibly on the detailed structure of the network of repulsive links. This explains the smooth transition in f_d as p_d grows. For large N, on the other hand, all sites in the network of repulsive links are statistically equivalent with respect to the distribution of negative links. Consequently, the transition takes always place at the same value of p_d, irrespectively of the specific realisation of the network. Accordingly, f_d exhibits a sharp growth from 0 to 1, which should become discontinuous in the thermodynamic limit. This semi-qualitative analysis sheds light on the role of the homogeneity of the distribution of negative links in defining the nature of the destabilisation transition of full synchronisation. This effect of the network structure on the collective dynamics of the system is further studied in the following.

3.2 Numerical study of the unsynchronised regime

In the fully synchronised state, the phases of all rotators are at the stable fixed point ϕ_s. The Kuramoto order parameter reaches its maximum value $\rho = 1$, whereas the absence of any kind of collective motion implies that both the Shinomoto-Kuramoto parameter ζ and the current J vanish. As full synchronisation breaks down, the parameter ρ is expected to decrease, and ζ and J can adopt non-zero values, as was shown in [7]. In this section, we present numerical results illustrating the behaviour of the order parameters as a function of the fraction of repulsive links p_d, for ensembles of different sizes, with $C = 4$, $\kappa = 10$, and $\omega = 0.98$.

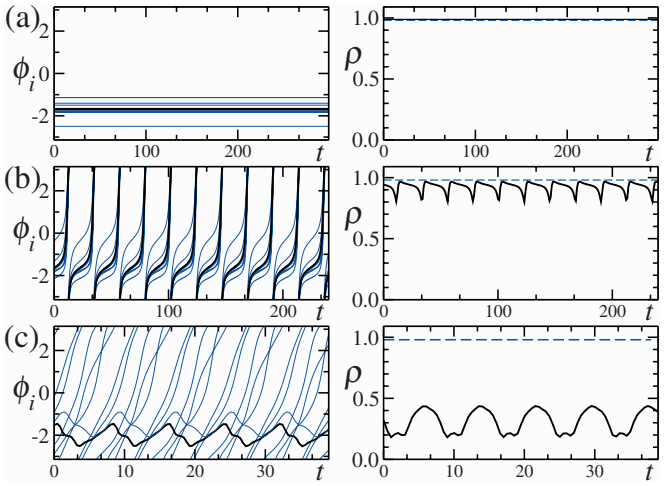

Fig. 2. Left column: time evolution of the collective phase $\Psi(t)$ (thick lines) and of the phases of ten representative rotators (thin lines) in an ensemble of size $N = 50$, for three values of the fraction of repulsive links: (a) $p_d = 0.015$, (b) 0.03, and (c) 0.1. The other parameters are $C = 4$, $\kappa = 10$, and $\omega = 0.98$. Right column: time evolution of $\rho(t)$, for the same realisations. The horizontal dashed line stands for the threshold of oscillatory behaviour, $\rho = \omega$ [7]. The middle panels correspond to the regime of global firing.

Figure 2 illustrates the dynamics of the rotator ensemble for three values of the fraction of p_d. Results correspond to numerical integration of equation (6) for a system of $N = 50$ rotators. In the left column, we show the time evolution of the collective phase $\Psi(t)$ together with that of ten representative rotators. In panel (b), which corresponds to an intermediate value of p_d, the rotators pulse in synchrony and, consequently, the collective phase performs periodic rotations. We identify this behaviour with the regime of global firing. In the right column, we show the evolution of the parameter $\rho(t)$, defined in equation (2), for the same realisations. The degree of synchronisation, measured by the time average of $\rho(t)$, decreases as the fraction of repulsive interactions grows.

In the three lower panels of Figure 1 we plot the order parameters ρ, ζ, and J as functions of the fraction of repulsive links. As expected, the decay in ρ is initially accompanied by growth in both ζ and J. As p_d increases, the current keeps growing indicating that, on average, the firing frequency of individual rotators is also increasing. The Shinomoto-Kuramoto parameter ζ attains a maximum at an intermediate value of p_d and then decreases. This is an indication that global synchronous firing occurs when full synchronisation is unstable and for moderate values of p_d. Larger fractions of negative links, however, make the dynamical coherence of the population decrease, and global firing becomes less distinct.

These results – in particular, the existence of and intermediate range of the probability p_d where global firing is most conspicuous – are in qualitative agreement with the collective behaviour of rotator ensembles where the disorder associated with repulsive interactions is replaced by noise and/or ensemble heterogeneity [7]. However, a noticeable quantitative difference resides in that, in the present case, the range of global firing becomes narrower as the system grows in size. The results of Figure 1 suggest that global firing may disappear for sufficiently large ensembles. An explanation for this collapse can be put forward recalling that the instability transition of full synchronisation becomes sharper as N grows (cf. the uppermost panel of Fig. 1). As discussed at the end of Section 3.1, for large systems, the number of repulsive links is statistically the same for all rotators. At the transition, all rotators abandon simultaneously the stable fixed point ϕ_s and, consequently, the ensemble adopts a highly disorganised phase configuration. In small systems, on the other hand, the transition is gradual. The stable fixed point is first abandoned by those rotators with a large number of repulsive links, which can be thus entrained into global synchronous firing.

This explanation indicates that, if it were possible to design a random network where the heterogeneity in the distribution of repulsive links is maintained as the system grows in size, the regime of global firing would persist for arbitrary large systems. In Section 4 we introduce a procedure to construct such a heterogeneous network, and numerically verify that the range where global firing occurs does not collapse as N grows. We also propose an interpolation between that kind of heterogeneous networks and Erdös-Rényi networks, and analyse global firing on these intermediate structures.

4 Heterogeneous networks

In this section, we introduce a method to construct a class of networks where the distribution of links per site preserves its heterogeneity as the size N increases. Specifically, the dispersion in the number of links per site is, in these networks, proportional to N so that the relative width of the distribution does not change with the size. According to the discussion at the end of Section 3, the effects of heterogeneity observed in small random networks of repulsive links, which disappear because of self-averaging in the random distribution of links, should persist in these new structures. In particular, we expect to find global firing even in large ensembles.

4.1 Construction of a heterogeneous network

To build up our heterogeneous network of repulsive links, we start by taking a random network of size N_0 and wiring probability p_d. The average number of links per site is $\bar{k}_0 \sim p_d N_0$, while its mean square dispersion is $\sigma_0 \sim \sqrt{p_d N_0}$. Let $\mathcal{N}_j$ be the set of the k_j neighbours of site j. We now consider M identical replicas of the starting network, which we use to build up a network of size $N = MN_0$. In each one of these replicas, say in replica m, we identify the site j_m which is homologous to the site j of the starting network. The M replicas are linked by connecting each site j_m with all the neighbours of all its homologous sites in all the replicas. In other words, the site j_m becomes linked to the $k_j M$ members of the sets $\mathcal{N}_{j_1}$, $\mathcal{N}_{j_2}$, ..., $\mathcal{N}_{j_M}$. Figure 3 illustrates the resulting network in a simple case. By construction, the number of neighbours of each site in the final structure equals M times the number neighbours of the homologous site in the starting network. Therefore, the average number of links per site and the mean square dispersion are, respectively,

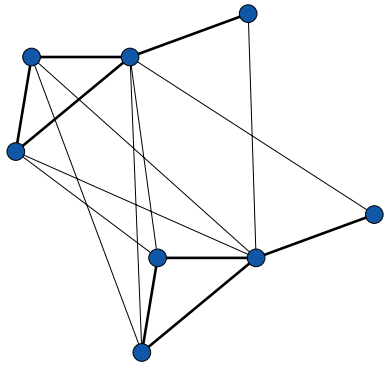

Fig. 3. A heterogeneous network constructed starting by a network of $N_0 = 4$ sites, and consisting of two replicas of the starting network. Bold lines stand for links inside each replica, and thin lines correspond to links connecting different replicas.

$$\bar{k} = M p_d N_0 = M \bar{k}_0 = p_d N, \tag{11}$$

and

$$\sigma = M\sigma_0 = N\sigma_0/N_0. \tag{12}$$

As advanced above, for fixed N_0, both the mean value and the dispersion in the distribution of links of the resulting network grow linearly with the number of sites N. The relative dispersion is thus independent of the network size.

Let $\mathbb{M}_0$ and $\mathbb{M}$ be the adjacency matrices of the starting network and the resulting network, respectively. It is possible to show that, if λ_0 is an eigenvalue $\mathbb{M}_0$, then $\lambda = M\lambda_0 = N\lambda_0/N_0$ is an eigenvalue of $\mathbb{M}$, with multiplicity N_0. The remaining eigenvalues are equal to zero. A similar relation holds for the matrix $\mathbb{N}$ of equation (8). This result differs from the prediction of the semicircle law, which stands for purely random matrices and states that $\lambda \sim \sqrt{N}$ [22]. Since, in equation (8), both $\mathbb{M}$ and $\mathbb{N}$ are divided by the network size N, the maximum eigenvalue of $\mathbb{J}$ – which is in turn determined by the maximum (positive) eigenvalue of $\mathbb{M}$ – does not depend on N. Thus, for fixed N_0, the critical point at which full synchronisation becomes unstable is independent of the size.

Clearly, the network resulting from our construction is not fully random. In fact, because of the interconnection of all the homologous sites, it can be shown to have a large clustering coefficient [21]. To interpolate between this structure and a fully random network, we introduce

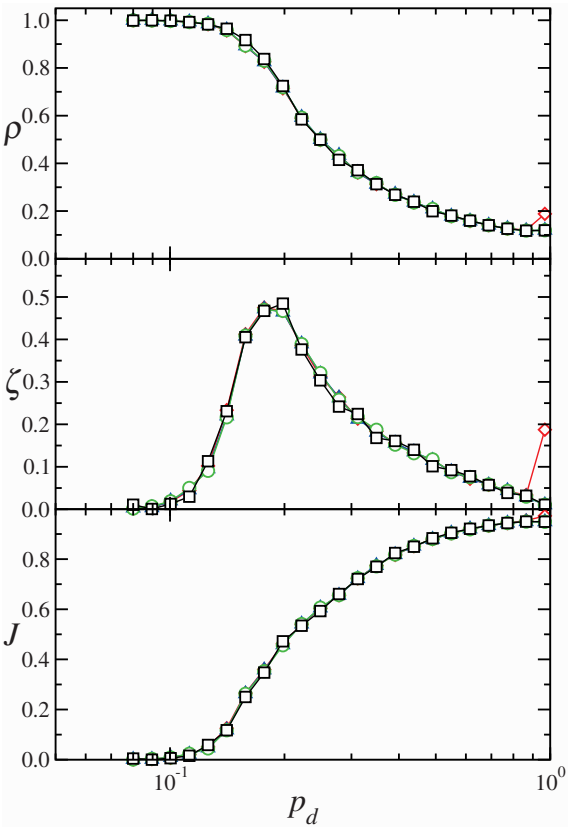

Fig. 4. The order parameters as functions of the fraction of repulsive links p_d, in the absence of rewiring, $p_f = 0$. Different curves, which are however practically coincident, correspond to sizes $N = 100$, 200, 400, and 1000. In all cases, the network of negative links is constructed from a starting network of $N_0 = 20$ sites. The other parameters are $C = 4$, $\kappa = 2$, and $\omega = 0.98$.

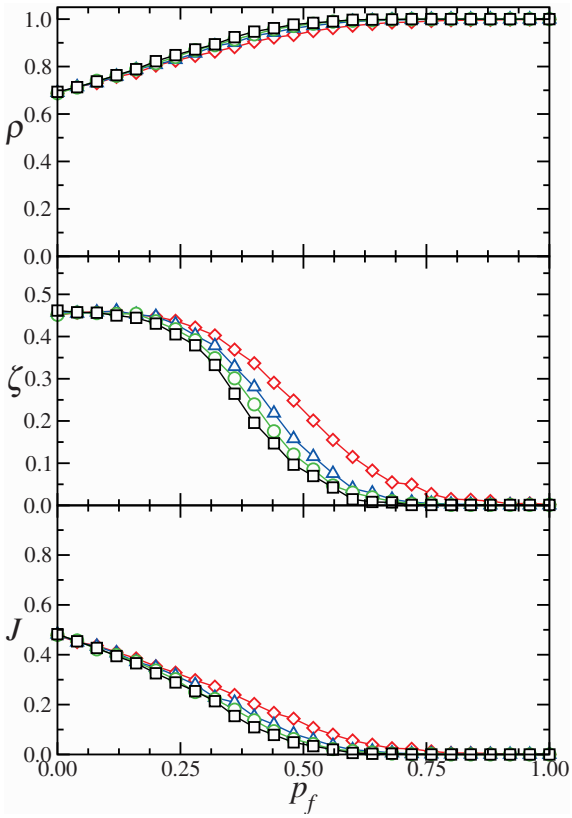

Fig. 5. The order parameters as functions of the rewiring probability p_f, for a fixed fraction of repulsive links, $p_d = 0.2$. Different curves correspond to sizes $N = 100$ ($\diamond$), 200 ($\triangle$), 400 ($\circ$), and 1000 ($\square$). In all cases, the network of negative links is constructed from a starting network of $N_0 = 20$ sites. The other parameters are $C = 4$, $\kappa = 2$, and $\omega = 0.98$.

a mechanism of link rewiring, in the spirit of small-world networks [23]. Starting from the heterogeneous network constructed above, we visit each site and, with probability p_f, rewire each of its links to a randomly chosen site all over the system. For $p_f = 1$, a fully random network is obtained. In the following, we study the collective behaviour of an ensemble of globally coupled rotators whose network of repulsive interactions is build as described here, in terms of the parameters p_d and p_f.

4.2 Numerical results

In our numerical analysis, the networks of repulsive links introduced in Section 4.1 are built starting from random networks of $N_0 = 20$ sites, and their final sizes are $N = 100$, 200, 400, and 1000. Also, we fix $C = 4$, $\kappa = 2$, and $\omega = 0.98$.

Figure 4 shows results for the order parameters ρ, ζ, and J as functions of the fraction of repulsive links p_d, in the absence of rewiring, $p_f = 0$. Different curves correspond to different sizes N. We see that, as expected, the order parameters are essentially independent of the system size. In particular, the regime of global firing – signalled, for intermediate values of p_d, by the maximum in the Shinomoto-Kuramoto parameter – clearly persists for large ensembles.

Figure 5 shows the order parameters as functions of the rewiring probability p_f, for a fixed fraction of negative links, $p_d = 0.2$ which corresponds, approximately, to the maximum common firing activity in the case $p_f = 0$, see Figure 4. The Shinomoto-Kuramoto parameter ζ is practically independent of N for small and large p_f, but exhibits a substantial dependence on the size for intermediate wiring probabilities. As may be expected from our results on Erdös-Rényi networks, in this intermediate zone, ζ is larger for smaller ensembles.

Finally, Figure 6 summarises the dependence of the order parameters on the probabilities p_d and p_f for an ensemble of $N = 400$ rotators. The graphs represent numerical results averaged over series of 100 realisation for each parameter set.

5 Conclusion

In this paper, we have shown that – like noise and ensemble heterogeneity [7] – structural disorder in a network of interacting excitable rotators can induce global firing

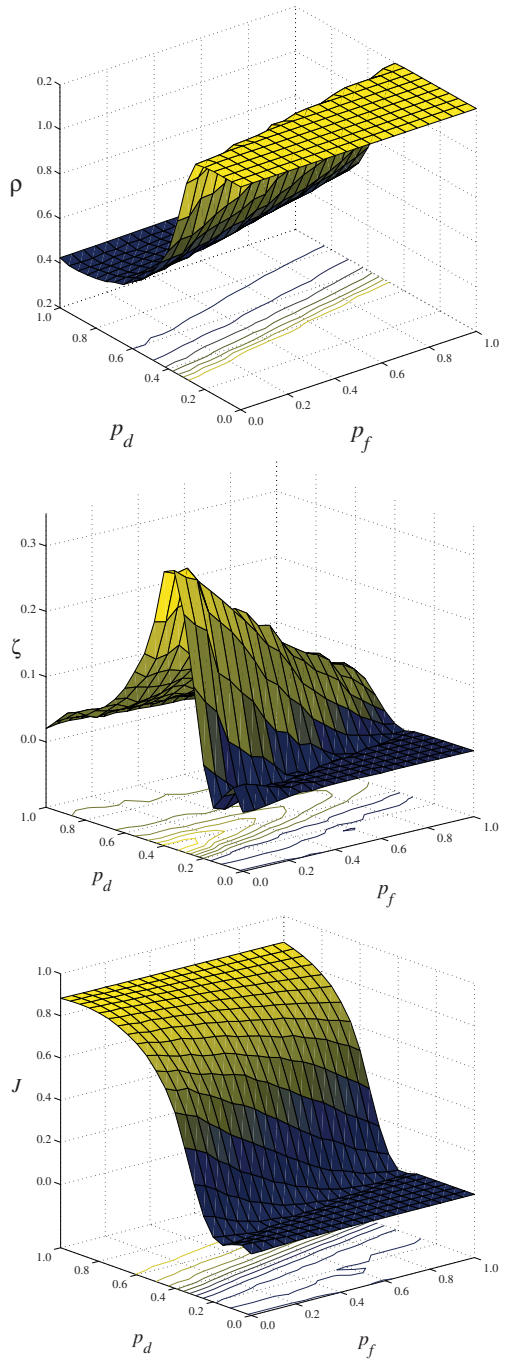

Fig. 6. The order parameters for an ensemble of $N = 400$ rotators ($N_0 = 20$) as functions of the fraction of negative links p_d and the rewiring probability p_f. The other parameters are $C = 4$, $\kappa = 2$, and $\omega = 0.98$.

of the ensemble. This form of collective dynamics is here a consequence of the presence of a fraction of repulsive couplings, randomly scattered all over the interaction network. These repulsive interactions destabilise the state of full synchronisation when their number and intensity are large enough. Just beyond this desynchronisation transition, for intermediate values of the fraction of repulsive couplings, the ensemble is entrained in a regime where many rotators are coherently excited, and global firing is triggered. While the results of this paper support the general mechanism for global firing put forward in [7], it is important to stress that the particular mechanism at work in the system studied here is quite different. In [7] the rotators showed heterogeneity in the form of dispersion in the natural frequencies ω_i. As the dispersion increased a fraction of the rotators had natural frequencies in the oscillatory range $\omega_i > 1$. Those rotators would spontaneously fire if they were isolated. When coupled, they pull the other rotators into an state of collective firing. In the system studied in this paper, on the other hand, the mechanism of destabilisation is produced by the effect that negative couplings have on individual rotators, but these would never fire if isolated. In both cases, however, it is the diversity, either in the natural frequencies or in the number of negative links, that produces the global effect. In fact, when the pattern of repulsive couplings forms an Erdös-Rényi random network the regime of global firing is progressively suppressed as the size of the ensemble grows. This effect can be ascribed to that, as the network becomes larger, there is self-averaging in its degree distribution, so that the number of neighbours per site becomes increasingly homogeneous. This homogeneity sharpens the desynchronisation transition and, at the same time, causes the collapse of the zone where global firing is possible for smaller systems. To avoid this effect of self-averaging – which clearly illustrates how increasing homogeneity can inhibit certain forms of coherent behaviour – we have introduced an algorithm to construct partially random networks whose degree distribution maintains its relative dispersion as the network grows. In this case, in fact, the order parameters which characterise the macroscopic behaviour of the rotator ensemble become essentially independent of the size. In particular, the regime of global firing persists for large systems.

The present results extend previous work on the effects of diversity of various origins over the collective dynamics of complex systems. These forms of diversity include now heterogeneous interaction patterns, with positive (attractive) and negative (repulsive) couplings. The extension is thus relevant to such systems as neural networks, where interactions of different signs are present in the form of activator and inhibitory synapses [10].

We acknowledge financial support from the MEC (Spain) and FEDER (EU) through projects FIS2006-09966, FIS2007-60327, the EU NoE BioSim LSHB-CT-2004-005137, and from CONICET and ANPCyT (Argentina) through projects PIP5114 and PICT04-943. CJT acknowledges financial support from SBF (Swiss Confederation) through research project C05.0148 (Physics of Risk).

References

1. J. García-Ojalvo, J.M. Sancho, *Noise in spatially extended systems* (Springer-Verlag, New York, 1999)
2. F. Sagués, J.M. Sancho, J. García-Ojalvo, Rev. Mod. Phys. **79**, 829 (2007)

3. R. Toral, C.J. Tessone, J. Viana Lopes, Eur. Phys. J. Special Topics **143**, 59 (2007)
4. L. Gammaitoni, P. Hänggi, P. Jung, F. Marchesoni, Rev. Mod. Phys. **70**, 223 (1998)
5. C.J. Tessone, C.R. Mirasso, R. Toral, J.D. Gunton Phys. Rev. Lett. **97**, 194101 (2006)
6. D.H. Zanette, Phys. Rev. E **64**, 050901R (2001); D.H. Zanette, Phys. Rev. E **65**, 041908 (2002)
7. C.J. Tessone, A. Scirè, R. Toral, P. Colet, Phys. Rev. E **75**, 016203 (2007)
8. Y. Kuramoto, *Chemical Oscillations, Waves, and Turbulence* (Springer, Berlin, 1984)
9. J.P. Keener, J. Sneyd, *Mathematical Physiology* (Springer, Berlin, 1988)
10. P. Dayan, L.F. Abbott, *Theoretical Neuroscience: Computational and Mathematical Modeling of Neural Systems* (MIT Press, Cambridge, 2001)
11. C.J. Tessone, E. Ullner, A. Zaikin, J. Kurths, R. Toral. Phys. Rev. E **74**, 046200 (2006)
12. H. Daido, Prog. Theor. Phys. **77**, 622 (1987)
13. H. Daido, Phys. Rev. Lett. **68**, 1073 (1992)
14. H. Daido, Phys. Rev. E **61**, 2145 (2000)
15. C. Zhou, A.E. Motter, J. Kurths, Phys. Rev. Lett. **96**, 034101 (2006)
16. D.H. Zanette, Europhys. Lett. **72**, 190 (2005)
17. S. Shinomoto, Y. Kuramoto, Prog. Theor. Phys. **75**, 1105 (1986)
18. P. Reimann, Phys. Rep. **361**, 57 (2002)
19. P. Erdös, A. Rényi, Publ. Math. (Debrecen) **6**, 290 (1959)
20. P. Erdös, A. Rényi, Publ. Math. Inst. Hung. Acad. Sci. **5**, 17 (1960)
21. R. Albert, L. Barabási, Rev. Mod. Phys. **74**, 47 (2002)
22. M.L. Mehta, *Random Matrices*, 2nd edn. (Academic Press, New York, 1991)
23. D.J. Watts, S.H. Strogatz, Nature **393**, 440 (1998)